Chemistry & Biology, Vol. 10, 341–349, April, 2003, ©2003 Elsevier Science Ltd. All rights reserved. DOI 10.1016/S1074-5521(03)00071-1

Crystal Structure of Human Carboxylesterase 1 Complexed with the Alzheimer's Drug Tacrine: from Binding Promiscuity to Selective Inhibition

Sompop Bencharit,[1,2] Christopher L. Morton,[4] Janice L. Hyatt,[4] Peter Kuhn,[5,6] Mary K. Danks,[4] Philip M. Potter,[4] and Matthew R. Redinbo[1,3,*]

[1]Department of Chemistry
[2]School of Dentistry
[3]Department of Biochemistry and Biophysics and The Lineberger Comprehensive Cancer Center
University of North Carolina, Chapel Hill
Chapel Hill, North Carolina 27599
[4]Department of Molecular Pharmacology
St. Jude Children's Research Hospital
Memphis, Tennessee 38105
[5]Stanford Synchrotron Radiation Laboratory
2575 Sand Hill Rd, MS 69
Menlo Park, California 94025

Summary

Human carboxylesterase 1 (hCE1) is a broad-spectrum bioscavenger that plays important roles in narcotic metabolism, clinical prodrug activation, and the processing of fatty acid and cholesterol derivatives. We determined the 2.4 Å crystal structure of hCE1 in complex with tacrine, the first drug approved for treating Alzheimer's disease, and compare this structure to the *Torpedo californica* acetylcholinesterase (AcChE)-tacrine complex. Tacrine binds in multiple orientations within the catalytic gorge of hCE1, while it stacks in the smaller AcChE active site between aromatic side chains. Our results show that hCE1's promiscuous action on distinct substrates is enhanced by its ability to interact with ligands in multiple orientations at once. Further, we use our structure to identify tacrine derivatives that act as low-micromolar inhibitors of hCE1 and may provide new avenues for treating narcotic abuse and cholesterol-related diseases.

Introduction

Human carboxylesterase 1 (hCE1) is a member of the serine hydrolase family of enzymes (E.C. 3.1.1.1) and exhibits low specificity and the ability to act on numerous structurally distinct substrates [1]. hCE1 hydrolyzes ester, thioester, and amide-ester linkages in a wide variety of endogenous and xenobiotic substrates [2, 3]. The enzyme is expressed in liver, intestine, kidney, lung, testes, heart, monocytes, and macrophages [2–4]. Its central biological role appears to be drug and xenobiotic metabolism necessary for the chemoprotective functions of proteins in the liver and other "front-line" defense tissues. hCE1 metabolizes numerous human drugs, including cocaine, heroin, meperidine, and lidocaine [5–7]. The enzyme also processes several prodrugs to their active forms in vivo, including the cholesterol-lowering drug lovastatin, and angiotensin-converting enzyme inhibitors delapril, imidapril, and temocapril [8, 9]. hCE1 employs the standard two-step serine hydrolase catalytic mechanism involving the formation of an acyl-enzyme intermediate at the enzyme's catalytic serine [2]. hCE1 shares 47% sequence identity with human intestinal carboxylesterase (hiCE; also called hCE2), a related esterase that exhibits substrate preferences distinct from hCE1 [4].

We have previously reported the first crystal structures of hCE1 in complexes with either the heroin analog naloxone methiodide or the cocaine analog homatropine [10]. These structures revealed that hCE1 exhibits the α/β-hydrolase fold typical of serine esterases but also contains a large substrate binding gorge with both rigid and flexible pockets. The hCE1 substrate binding gorge is lined largely by hydrophobic residues which surround a serine esterase catalytic triad composed of Ser-221, His-468, and Glu-354. In addition, we showed that hCE1 exists in a trimer-hexamer equilibrium that can be shifted toward trimer through the binding of compounds to a site on the surface of the enzyme. hCE1 metabolizes the methyl ester linkage on *R*-cocaine, and both acetyl groups on heroin to generate 6-acetylmorphine and morphine [5, 11]. hCE1 is also capable of *trans*-esterifying cocaine in the presence of ethanol to cocaethylene, a toxic cocaine metabolite found in humans when cocaine and alcohol are abused together [12]. *trans*-esterification occurs when ethanol attacks the covalent acyl-enzyme intermediate rather than water. Regulating hCE1's activity during situations of narcotic abuse or overdose could provide a novel way to treat these conditions.

hCE1 also appears to be involved in cholesterol trafficking and other processes important to cell biology and human physiology. hCE1 contains fatty acyl ethyl ester (FAEE) synthase activity in which long-chain fatty acids are *trans*-esterified with ethanol to generate FAEEs [13]. The build-up of these toxic compounds in the tissues of alcoholics is a hallmark of the development of this disease and is thought to play a role in the necrotic action of ethanol in liver and other organs [14]. hCE1 has also been reported to contain both acyl-coenzyme A:cholesterol acyl transferase (ACAT) activity [15], which creates cholesteryl esters, and cholesteryl ester hydrolase (CEH) activity [16]. These actions are important for cholesterol trafficking both within cells and between tissues throughout the body. hCE1 was recently found to be one of only three cellular targets bound by the anticancer drug tamoxifen, and it was proposed that the physical interaction between tamoxifen and hCE1 may mediate the cholesterol-lowering effects of this drug [17].

In additional to its catalytic actions, hCE1 appears to be critical to protein retention and release from the endoplasmic reticulum (ER) [18]. hCE1 contains ER targeting and retention sequences at its N and C termini, respectively, and associates with the ER lumen [19]. When it traffics to the surface of hepatocytes for secretion into circulating plasma, hCE1 is one of the proteins

*Correspondence: redinbo@unc.edu
[6]Present Address: Department of Cell Biology, The Scripps Research Institute, Scripps PARC Institute, CB227, 10550 North Torrey Pines Road, La Jolla, California 92037.

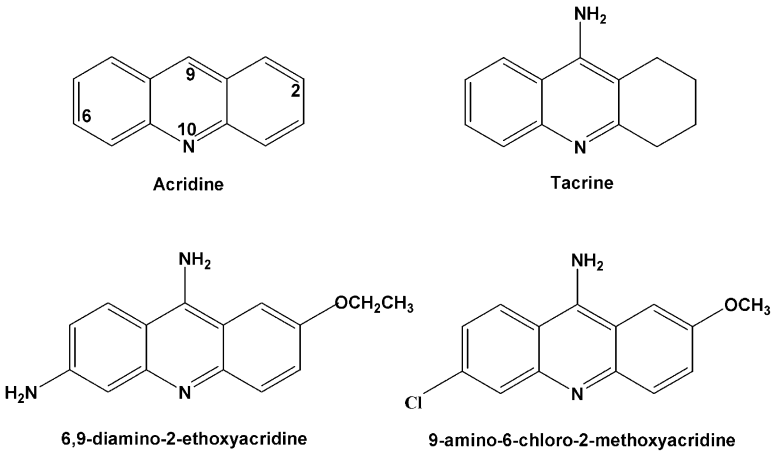

Figure 1. Chemical Structures of Acridine, Tacrine, 6,9-Diamino-2-Ethoxyacridine, and 9-Amino-6-Chloro-2-Methoxyacridine, with the Acridine Numbering System Indicated

the sporozite stage of the *Plasmodium falciparum* parasite interacts with to gain entrance into liver cells [20]. hCE1 (also called egasyn) complexes with the UDP-glucuronysyltransferase (UGT) phase II drug metabolism enzymes to hold the UGT's in the ER lumen [21]. hCE1 is also involved in binding to and retaining the C-reactive protein (CRP) in the ER lumen of human hepatocytes [22]. CRP responds to infection and cellular damage throughout the body and was recently identified as a highly sensitive early marker of cardiovascular disease [23].

Tacrine (9-amino-1,2,3,4- tetrahydroacridine) was the first drug approved for the treatment of the symptoms of Alzheimer's disease (AD; Figure 1) [24]. Tacrine is a potent inhibitor (Ki = 38 nM) [25, 26] of human acetylcholinesterase (hAcChE), another serine hydrolase related in sequence (30% identity) and structure (1.2 Å rmsd over 532 Cα positions) to hCE1. The clinical action of tacrine in alleviating symptoms of AD is thought to occur by inhibiting hAcChE and prolonging the lifetime of the acetylcholine neurotransmitter in human brain. The effectiveness of this treatment, however, has been challenged by recent clinical studies [27, 28].

We sought to elucidate the differences in ligand binding between hCE1, a low-specificity enzyme, and hAcChE, a high-specificity enzyme, in complex with the same compound. We present the crystal structure of hCE1 in complex with tacrine and compare it to the *Torpedo californa* AcChE-tacrine complex [29, 30]. Our results show that hCE1 enhances its ligand binding promiscuity by using a large and conformable active site that is capable of allowing compounds to dock in several different orientations at once. We further describe tacrine analogs that act as low-micromolar inhibitors of hCE1.

Results

Overall Structure

The structure of hCE1 in complex with tacrine was refined to 2.4 Å resolution using torsion angle dynamics and the maximum likelihood target implemented in CNS (Table 1). The asymmetric unit contains one hexamer with 32 point group symmetry formed by two stacked C3 trimers (Figures 2A and 2B). The hCE1-tacrine trimer is similar to the structures of hCE1 in complexes with the cocaine analog homatropine and the heroin analog naloxone reported previously, sharing 0.35 and 0.33 Å rmsd over all equivalent atoms, respectively [10]. Each hCE1 monomer is composed of a central catalytic domain, which contains the serine hydrolase catalytic triad, an α-β domain, and a regulatory domain (Figure 2A). The active site is located at the base of a 10–15 Å deep catalytic gorge formed at the interface of the three domains, and is covered by two loops, Ω1 and Ω2, and two helices, α1 and α10′. The enzyme contains two disulfide linkages per monomer (87–116, 274–285), as well as one high-mannose N-linked glycosylation site at

Table 1. Crystallographic Statistics for the hCE1-Tacrine Complex

Data Collection	
Resolution (Å; highest shell)	25–2.4 (2.42–2.4)
Space group	$P2_1$
Asymmetric unit	one hexamer
Cell constants (Å, °)	a = 90.0
	b = 117.0
	c = 176.0
	α = 90
	β = 95.7
	γ = 90
Total reflections	563,091
Unique reflections	141,078
Mean redundancy	4.0
R_{sym}[a] (%; highest shell)	8.1 (23.1)
Wilson B factor (Å^2)	35.4
Completeness (%; highest shell)	99.5 (99.9)
Mean I/σ (highest shell)	14.3 (5.1)
Refinement Statistics	
R_{cryst}[b] (%; highest shell)	16.2 (21.2)
R_{free}[c] (%; highest shell)	20.7 (28.2)
Number protein atoms	24,756
Number solvent sites	2,505
Number carbohydrate atoms	176
Number ligand atoms	90

[a] $R_{sym} = \Sigma|I - <I>|/\Sigma I$, where I is the observed intensity and $<I>$ is the average intensity of multiple symmetry-related observations of that reflection.

[b] $R_{cryst} = \Sigma||F_{obs}| - |F_{calc}||/\Sigma|F_{obs}|$, where F_{obs} and F_{calc} are the observed and calculated structure factors, respectively.

[c] $R_{free} = \Sigma||F_{obs}| - |F_{calc}||/\Sigma|F_{obs}|$ for 7% of the data not used at any stage of structural refinement.

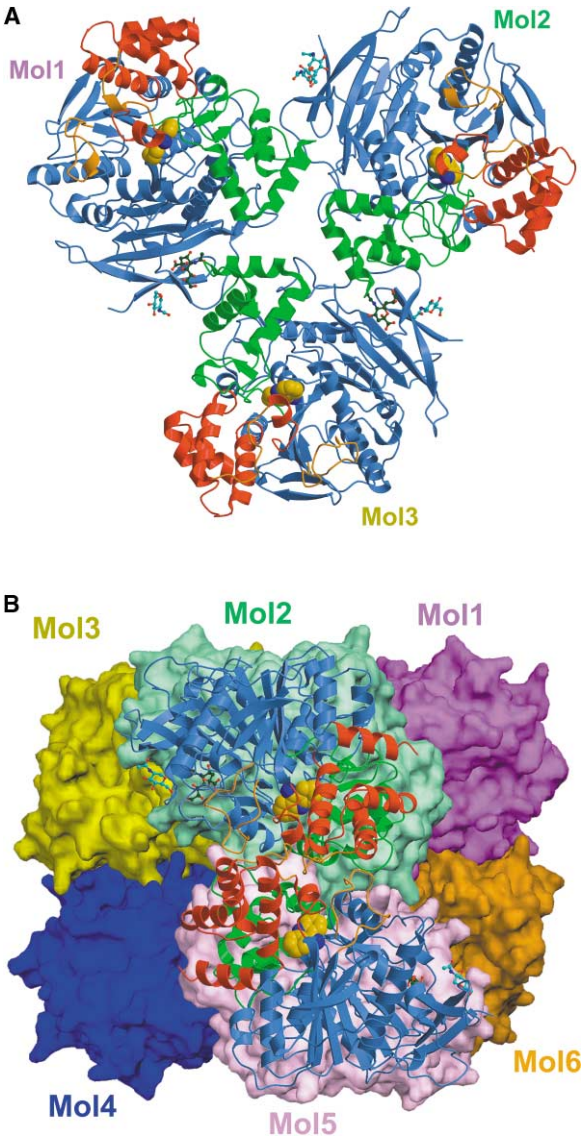

Figure 2. Structure of the Human Carboxylesterase 1-Tacrine Complex

(A) A trimer of hCE1 (MOL1, MOL2, and MOL3) complexed with tacrine viewed down the 3-fold axis of symmetry and into the catalytic gorge of each monomer. The catalytic domains, $\alpha\beta$ domains, and regulatory domains of each monomer are in blue, green, and red, respectively, the novel Ω loops are in orange, the N-acetylglucosamines (NAG) are in cyan, and the sialic acids (SIA) are in dark green.

(B) A molecular surface representation of the hCE1 hexamer with a ribbon representation of one pair of dimers within the hexamer superimposed. The hCE1 hexamer is formed by the stacking of two trimers with their active sites facing in. The hCE1 monomers are labeled MOL1 to MOL6.

Asn-79. One or two N-acetylglucosamines (NAG) were traced at each of the six glycosylation sites in the asymmetric unit. In addition, in three of the six monomers, a sialic acid moiety (SIA) was identified and found to pack against the N terminus of α7 in an adjacent monomer in the hCE1 trimer. Although these SIA moieties are not connected to the NAGs by clear electron density, we expect that they are the portions of a long glycosylation site present at each Asn-79. They appear to assist in the stabilization of the hCE1 trimer by packing into adjacent monomers in the oligomer.

The hCE1 hexamer is formed by two trimers stacked together with their substrate binding gorges facing toward one another (Figure 2B). While the hCE1 trimer buries only 475 Å^2 of solvent-accessible surface area per monomer, the dimer interface that creates the hexamer is more extensive, burying 1900 Å^2 of surface area per monomer. A critical packing interaction stabilizing the hexamer is the interdigitation of the Ω1 and Ω2 loops that creates the "Z site." In the structure of hCE1 complexed to the cocaine analog homatropine, the Z site was found to bind to an enantiomeric mixture of homatropine molecules, and these prevent the packing of the hexamer. Thus, the hCE1-homatropine complex contained only trimers in the asymmetric unit [10]. In the hCE1-tacrine structure, however, the Z site is not filled by ligand, but instead forms a dimeric interface critical to creating the hCE1 hexamer.

Interpreting Electron Density at the Active Site

hCE1 was crystallized in the presence of 100-fold molar excess tacrine. After structural refinement of the protein, carbohydrate, and solvent models was complete, we calculated 2.4 Å resolution simulated annealing (SA) omit maps at the active site of each hCE1 monomer. It was clear from these electron density maps that tacrine was bound within each substrate binding gorge (Figure 3). The density at the active sites was planer and of roughly the correct size and shape for the planer tacrine ligand. It was also clear, however, that tacrine was present in multiple orientations at each active site. When single orientations of tacrine were placed within SA omit density, they did not fill all the electron density preset. Further, when these single orientations were refined, positive difference electron density peaks of 5–8 σ appeared, indicating the presence of additional atoms at each active site. When water molecules were found to be insufficient to satisfy this difference density, we pursued the placement of additional tacrine ligands at each active site. We used a combination of SA omit density, difference density, and the program Blob, which uses a Monte Carlo algorithm to place ligands into electron density, to interpret the density at each active site [31]. The density in some monomers was clearer than in others. For example, monomers 1 and 4 indicated that the 9 amino group on tacrine can be placed up away from the catalytic Ser-221 residue (Figures 3A and 3D), while in monomers 2 and 6 this placement of the 9 amino group was not observed (Figures 3B and 3F).

We placed four or five tacrine molecules per protein monomer in our final model: monomer 1 has four tacrines (Figure 3A), monomer 2 has four tacrines (Figure 3B), monomer 3 has five tacrines (Figure 3C), monomer 4 has five tacrines (Figure 3D), monomer 5 has five tacrines (Figure 3E), and monomer 6 has four tacrines (Figure 3F). Note that the tacrine ligand has pseudo 2-fold symmetry perpendicular to the molecule's long axis, which relates the aromatic and nonaromatic rings of the compound (Figure 1). This was one source of the ambiguity in ta-

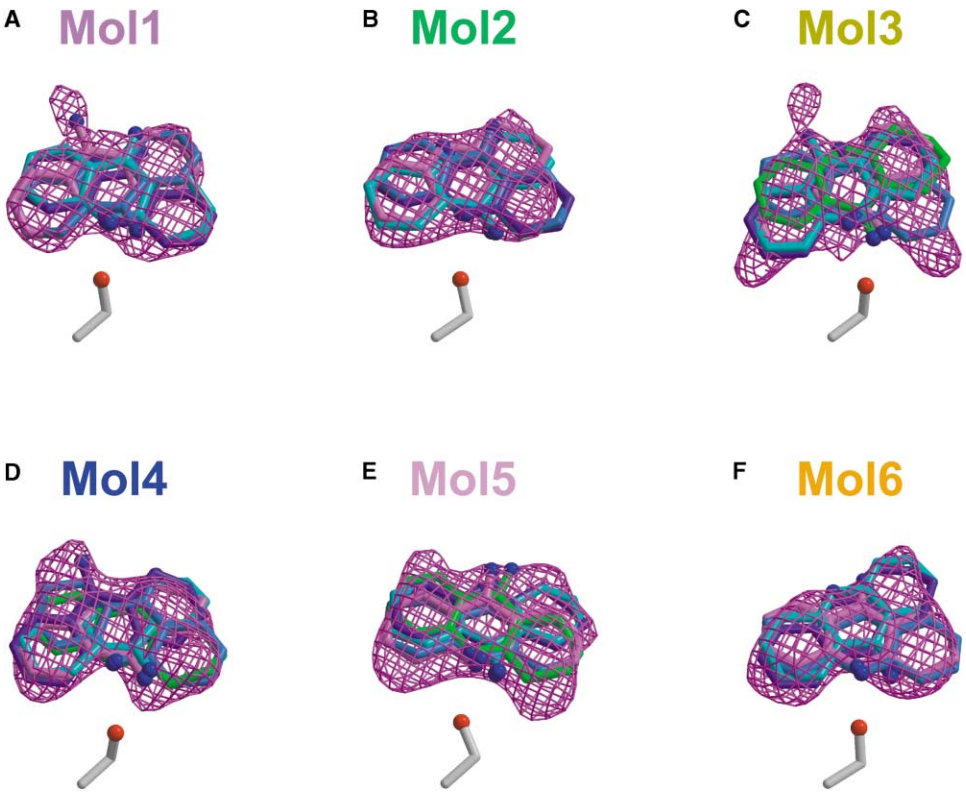

Figure 3. 2.4 Å Resolution Simulated Annealing Omit Maps (Contoured at 3.0 σ) Showing the Electron Density for Tacrine Bound at Each Active Site of the hCE1 Hexamer

The Cα, Cβ, and Oγ atoms of the catalytic Ser-211 residue are also shown in each panel. We identified four tacrine binding conformations in monomers 1 ([A]; MOL1), 2 ([B]; MOL2), and 6 ([F]; MOL6), and five tacrine binding conformations in monomers 3 ([C]; MOL3), 4 ([D]; MOL4), and 5 ([E]; MOL5).

crine's binding to the hCE1 active site. It was difficult to judge whether the nonaromatic ring was to be to the left or the right of Ser-221 (as viewed in Figure 3). In addition, tacrine has a secondary amine (at the 10 position) that serves as a hydrogen bond acceptor and a primary amine (at the 9 position) that serves as a hydrogen bond donor. Because Ser-221 acts as both a hydrogen bond donor and acceptor, it was difficult to interpret whether the primary or secondary amine lay adjacent to this polar residue at the active site. This generated a second ambiguity in tacrine's binding to hCE1, although Ser-221 forms hydrogen bonds of between 2.5–3.7 Å long with either the primary or secondary amines in all the tacrine binding modes identified. Each of these factors played a role in the placement of a constellation of ligands into the SA omit electron density at the active sites of hCE1 monomers. Our final model of describing the binding of four or five tacrine molecules per enzyme appears to validate effectively the ligand interaction, as no difference electron density peaks less than −1.0 σ or greater than 2.0 σ were present after refinement.

Tacrine Binding at the hCE1 Active Site

In spite of the multiple binding modes observed for tacrine in each hCE1 monomer, the ligands make several contacts conserved in all six active sites. First, either the 9 amino primary amine or the secondary ring amine at the 10 position of tacrine forms a hydrogen bond with the side chain of the catalytic Ser-221 residue (Figure 4). The primary amine contacts Ser-221 in 16 of the 27 observed binding modes, while the secondary amine contacts it in the remaining 11 modes (Figures 3 and 4). Second, the position of the polar nitrogen group of tacrine is somewhat variable depending on the binding mode, shifting by up to 3 Å between binding modes but always maintaining hydrogen bond distance from Ser-221 (Figures 3 and 4). It can be said that tacrine appears to "float" around Ser-221 within the hCE1 active site. For this reason, the noncentral rings of tacrine can adopt several positions within the substrate binding pocket. The ensemble of tacrines is butterfly shaped in several active sites, and these assemblies fill the large hCE1 binding gorge more effectively than a single ligand orientation would (Figures 3 and 4). The relatively nonpolar rings of tacrine contact hydrophobic amino acid side chains that line the substrate binding gorge of hCE1. Residues that interact with these regions of tacrine include Leu-97, Phe-101, Leu-255, Leu-318, Leu-358, Leu-363, Met-364, Leu-388, Met-425, and Phe-426. These rings are observed to dock within both the small, rigid pocket of hCE1's active site (adjacent to Phe-101), and the large, flexible pocket (adjacent to Leu-255) [10]. The ability of hCE1 to allow tacrine to dock in multiple orientations at once is likely due to several factors, including

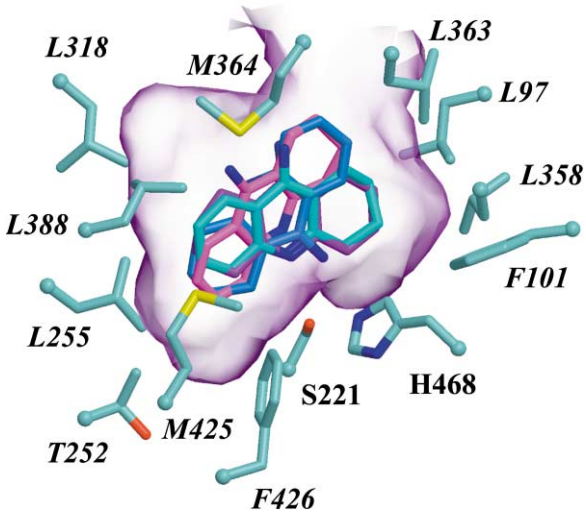

Figure 4. Four Binding Modes of Tacrine Bound within the Catalytic Pocket of hCE1 MOL1

The protein residues that line this catalytic pocket are in light blue, along with the catalytic residues (labeled in bold). The molecular surface of the catalytic binding pocket is rendered in transparent purple.

the enzyme's large binding pocket, tacrine's relatively small size, and its pseudo-symmetry.

Comparison between Tacrine Binding to hCE1 and AcChE

We compared structure of tacrine complexed with the *Torpedo californica* (eel) acetylcholinesterase (AcChE) [29, 30] to the hCE1-tacrine complex. hCE1 and AcChE both exhibit the α/β hydrolase fold common to serine hydrolases, and share 38% sequence identity and 1.23 Å rmsd over 429 equivalent Cα positions (Figure 5A). The most significant structural differences between the two enzymes occur in two regions—at the putative "back door" region of AcChE and within the substrate binding gorge. The "back door" was proposed to be a secondary product exit site for the AcChE's and to be gated by Trp-84 on the catalytic domain of the enzyme [32, 33]. hCE1 places a Phe-101 perpendicular to the position of Trp-84 in AcChE, effectively blocking the back door in hCE1.

At the active site, the serine hydrolase catalytic triads of both enzymes line up well (Figure 5B). However, hCE1 creates a larger substrate binding gorge that packs within a distinct region of the enzyme relative to AcChE. As described above, hCE1's binding gorge is lined by hydrophobic and, in some cases, mobile amino acid side chains [10], and allows tacrine to bind in up to five orientations at once. AcChE, in contrast, frames a smaller ligand binding pocket with largely aromatic side chains, including Trp-84, Tyr-121, Trp-279, Phe-290, Phe-330, Phe 331, Tyr-334, and Trp-432 (Figure 5B). AcChE docks tacrine in a single, specific orientation between Trp-84 and Phe-330, two aromatic side chains conserved in all AcChE enzymes examined to date. Tacrine largely fills the available space in the AcChE binding pocket, offering room for small substituent groups that improve binding affinity [25, 26, 29, 30]. Further, AcChE tacrine binding site is 6 Å from that in hCE1 (the distance between the 9 amino positions was measured). Thus, hCE1 and AcChE bind to tacrine in distinct ways and using discrete binding pockets in each case. These observations explain why tacrine is a nanomolar affinity inhibitor of AcChE and does not inhibit hCE1 up to concentrations of 100 μM.

Selective, Tacrine-Based Inhibitors of hCE1

Selective hCE1 inhibitors will be useful tools to examine the function of this enzyme in vitro and in vivo. Based on our crystal structure of hCE1 in complex with tacrine, we hypothesized that the presence of small substituent groups at the 2 and 6 positions of tacrine would improve the binding affinity of the compound for hCE1 (Figure 5B). We identified two commercially available analogs of tacrine that contain substitutions on the 2 and 6 positions: 6,9-diamino-2-ethoxyacridine and 9-amino-6-chloro-2-methoxyacridine (Figure 1). These compounds are based on the acridine scaffold, which is identical to tacrine except that all rings are aromatic. We examined the inhibitory effects of these compounds and tacrine on hCE1, hAcChE, and hiCE. hiCE (also called hCE2) shares 47% sequence identity with hCE1, is present largely in intestine and liver, and exhibits preferences for distinct substrates relative to hCE1. We found that whereas tacrine is not an inhibitor of hCE1, 6,9-diamino-2-ethoxyacridine and 9-amino-6-chloro-2-methoxyacridine inhibited hCE1 with Ki's of 17.1 and 5.8 μM, respectively (Table 2). This represents an improvement of $>$10-fold over tacrine's ability to inhibit hCE1. We further found that 6,9-diamino-2-ethoxyacridine and 9-amino-6-chloro-2-methoxyacridine served as weaker inhibitors of hAcChE relative to tacrine (Table 2). This was expected because there appears to be little room for these substituent groups in the AcChE substrate binding gorge. Neither tacrine, 6,9-diamino-2-ethoxyacridine nor 9-amino-6-chloro-2-methoxyacridine inhibited hiCE (Table 2), further supporting the conclusion that this enzyme is distinct from hCE1 in its substrate binding gorge [4]. In summary, we show that the addition of small, substituent groups onto the tacrine scaffold produce selective, low-micromolar inhibitors of hCE1.

Discussion

Variation in cholesterol trafficking at the blood-brain barrier has been shown to be an important factor in the development of Alzheimer's disease [34]. Because hCE1 appears to play a role in cholesterol trafficking [13, 15], we sought to examine the enzyme's ligand binding promiscuity and to identify novel hCE1 inhibitors useful for both in vitro and in vivo studies. We found using combined crystallographic and biochemical studies that hCE1 allows tacrine to bind within its large substrate binding gorge in multiple orientations at once, that hCE1 and AcChE bind to tacrine in distinct ways, and that simple tacrine analogs are selective hCE1 inhibitors. Similar structural and biochemical studies may allow

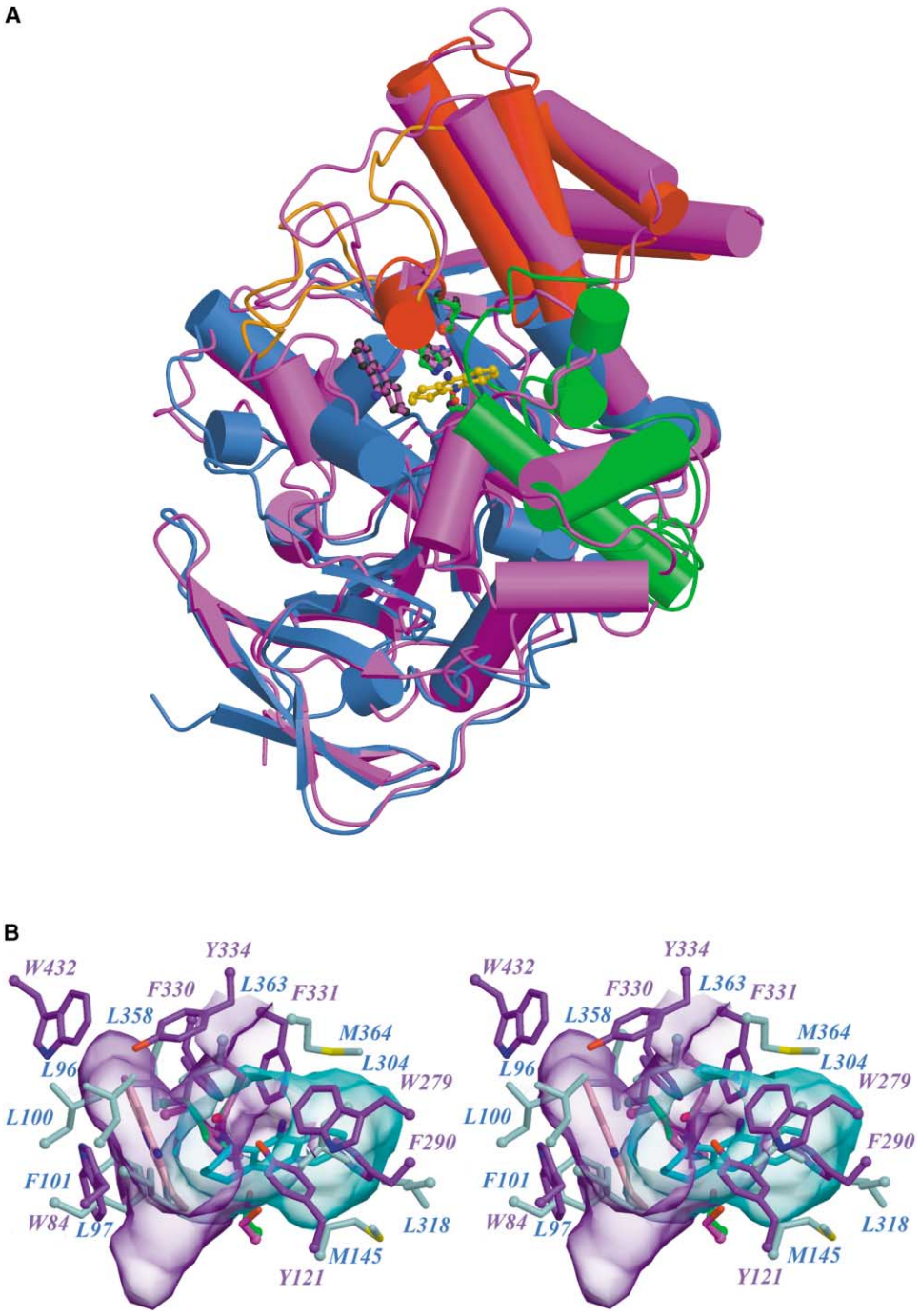

Figure 5. Human Carboxylesterase 1 and Acetylcholinesterase

(A) The hCE1-tacrine complex superimposed on the *Torpedo californica* AcChE-tacrine complex (magenta; PDB code 1ACJ). hCE1 (MOL1) is colored by domains as in Figure 2A, with the bound tacrine in yellow.

(B) Stereoview of the catalytic gorges of hCE1 and *Torpedo californica* AcChE superimposed. The molecular surface of ligand binding cavities of hCE1 and AcChE are rendered in transparent cyan and purple, respectively. The catalytic triad of hCE1 (green) and AcChE (magenta) superimpose well. The residues lining the hCE1 binding cavity (light blue) are largely hydrophobic and aliphatic, while those lining the AcChE binding cavity (purple) are aromatic. Note that the shapes of the binding cavities and the locations of the ligands within them are distinct. In the hCE1 structure, tacrine (cyan) contacts aliphatic residues and forms one hydrogen bond with the enzyme's catalytic serine. In AcChE, however, tacrine (light purple) stacks between Trp-84 and Phe-330.

the design of novel compounds for the management of cholesterol homeostasis in humans.

The tacrine scaffold has been extensively examined using structure-activity relationships, and several novel tacrines have been identified that inhibit hAcChE [24, 35–37]. Among the most elaborate are the bis-tacrines in which two tacrine compounds are linked by six to eight carbons between the 9 amino positions [36]. These

Table 2. Selective Inhibition of Human Carboxylesterase 1

	hCE1	hiCE	AcChE
Tacrine	>100 μM	>100 μM	6.9 nM
6,9-diamino-2-ethoxyacridine	17.1 μM	>100 μM	0.49 μM
9-amino-6-chloro-2-methoxyacridine	5.8 μM	>100 μM	49 nM

Ki values for the inhibition of hCE1, hiCE, and human AcChE by the compounds listed.

compounds (which are not commercially available) inhibit hAcChE by placing two tacrines within the catalytic gorge of the enzyme, one at the base (cation-Π site) and one at the rim (peripheral site) [38]. The protein dimer essential to the hCE1 hexamer positions the catalytic gorges of hCE1 in close proximity, only ~3–4 Å apart or ~36 Å between the catalytic Ser-221 of the dimeric partners (Figure 2B). It would be of interest to examine the effect that bis-tacrines connected by linkers of ~30–40 Å would have on the activity and oligomerization state of hCE1. It is possible that such compounds will be inhibitors of hCE1 and will shift the hCE1 trimer-hexamer equilibrium toward hexamer, allowing one to examine the impact hCE1 activity and oligomerization state have on various biological functions.

hCE1 joins other proteins and enzymes that are promiscuous in terms of either ligand or substrate binding. Promiscuous proteins of known structure include rabbit cytochrome P450 2C5 (CYP2C5) [39], the human xenobiotic nuclear receptor PXR [40], and the bacterial quorum sensor (QacR) [41]. The latter two proteins are transcriptional regulators that act as front-line detectors of xenobiotic stress, while CYP2C5 performs oxidative metabolism on structurally distinct compounds including progesterone and several steroid compounds. Certain elements common to each of these proteins help to identify characteristics involved in ligand binding promiscuity. First, hCE1, PXR, CYP2C5, and QacR all allow ligand to bind in multiple orientations at once, or to several sites on the protein. Second, each protein uses a large and structurally flexible ligand binding pocket that expands the chemical space it can sample. Indeed, these binding pockets appear to encourage the shuffling of ligand-protein interactions to enable the binding of multiple ligand orientations simultaneously. Third, because CYP2C5, PXR, and hCE1 tend to bind to hydrophobic ligands, each protein lines their ligand binding pocket with largely hydrophobic side chains, but also offers a few polar residues to allow for hydrogen bonds. In general, these proteins appear to favor hydrophobic, van der Waals, and hydrogen bonding interactions over electrostatic contacts when possible. Taken together, these characteristics help to elucidate some of the ways proteins may have sacrificed binding affinity and selectivity for the broader spectrum ability to recognize and act on numerous structurally distinct compounds. hCE1 appears to employ this substrate binding promiscuity for both chemoprotective functions and endogenous roles in several biological processes.

Significance

Human carboxylesterase 1 (hCE1) is a broad-spectrum bioscavenger that plays important roles in narcotic metabolism, the activation of clinical prodrugs, and the processing of fatty acid and cholesterol derivatives in liver and other tissues. Tacrine (9-amino-1,2,3,4-tetrahydroacridine) is a potent inhibitor of human acetylcholinesterase (hAcChE), an enzyme related in structure and mechanism to hCE1, but does not inhibit hCE1 up to 100 μM. To unravel differences in ligand binding between the low-specificity hCE1 and high-specificity AcChE enzymes, we determined the 2.4 Å crystal structure of hCE1 in complex with tacrine (using 10 mM concentrations of the drug) and compare this structure to the *Torpedo californica* AcChE-tacrine complex. hCE1 allows tacrine to bind in multiple orientations within the large active site of each protein monomer in the hCE1 hexamer. Tacrine docks within the center of the hCE1 catalytic gorge and is contacted by several hydrophobic side chains, while it stacks in the smaller AcChE active site between two aromatic side chains. A high concentration of the tacrine was required to visualize the drug bound to the enzyme. However, using our structure, we identify two acridine analogs, which are related in structure to tacrine, and show that they act as low-micromolar inhibitors of hCE1. The development of selective inhibitors of hCE1 may provide new avenues for treating narcotic abuse and cholesterol-related diseases.

Experimental Procedures

Protein Purification and Crystallization

A secreted, 62 kDa form of hCE1 was expressed using baculovirus in *Spodoptera frugiperda* Sf21 cells and purified as described [42, 43]. hCE1 was concentrated to 3 mg ml^{-1} in 50 mM HEPES (pH 7.4) and crystallized in the presence of 10 mM tacrine using sitting drop vapor diffusion at 22°C. Crystals of 200–300 μm in size grew in 10% PEG-3350, 0.4 M Li_2SO_4, 0.1 M NaCl, 0.1 M LiCl, 0.1 M citrate (pH 5.5), and 5% glycerol, and were cryo-protected in 15% sucrose plus mother liquor prior to flash cooling in liquid nitrogen.

Structure Determination and Refinement

Diffraction data were collected at Stanford Synchrotron Radiation Laboratory (SSRL) beamline 9-1 at 100 K using cryo-cooled crystals and were processed and reduced using HKL2000 [44]. The hCE1-tacrine complex structure was determined by molecular replacement (AMoRe) [45] using the 2.8 Å structure of hCE1 in complex with the cocaine analog homatropine (RCSB code 1MX5) [10] as a search model. The structure was refined without carbohydrate groups, ligands, or waters using torsion angle dynamics in CNS [46] with the maximum likelihood function target, and included an overall anisotropic B factor and a bulk solvent correction. Seven percent of the observed data were set aside for cross-validation using free R prior to any refinement. Noncrystallographic symmetry restraints were employed at initial refinement stages and then removed such that each monomer was refined independently. Manual adjustments were performed using the program O [47] and σ_A-weighted [48] electron density maps. N-linked glycosylation sites were traced in all monomers. Simulated annealing difference density of >4 σ frequently indicated the presence of an additional sialic acid sugar moiety located 4–7 Å from the first N-acetylglucosamines of the

N-linked glycosylation sites at Asn-79. These sialic acid sugars are not connected by clear density to the carbohydrate chain; however, they appear to stabilize the hCE1 trimer by packing against a neighboring protein monomer.

Simulated annealing difference density maps indicated the presence of multiple orientations of tacrine within the active sites of each hCE1 monomer (Figure 4). The program Blob [31], which fits ligands into experimental electron density, was used to guide the placement of additional orientations of tacrine molecules. Three of six monomers contain four tacrine orientations, and the remaining three monomers contain five tacrine orientations. Final structures exhibit good geometry with no Ramachandran outliers. Molecular graphic figures were created with MolScript [49], BobScript [50], Raster3D [51], and Dino (www.dino3d.org).

Enzyme Inhibition Assays

Carboxylesterases

Determination of Ki values was performed for the CEs using 3 mM o-nitrophenyl acetate as a substrate. Briefly, inhibition constants were calculated by assessment of the reduction in the formation of o-nitrophenol, as monitored by a spectrophotometric assay at 420 nm, using purified hCE1 and hiCE [42, 52, 53]. Reactions were performed in 96-well plates in a total volume of 200 μl of 50 mM HEPES (pH 7.4), and data was recorded at 15 s intervals for up to 5 min. All reactions were performed in duplicate, and at least eight concentrations of inhibitor were used to determine Ki constants. Enzyme velocity values versus inhibitor concentrations were plotted, and Ki values were calculated from sigmoidal curve fits using GraphPad Prism software and established methods [54]. Routinely all curve fits demonstrated r^2 values of 0.95 or greater.

Acetylcholinesterase

Purified human acetylcholinesterase (hAcChE) was purchased from Sigma (C-0663, amphiphilic form purified from human erythrocytes) in 20 mM HEPES (pH 8.0) containing 0.1% Triton X-100, was stored at 4°C, and was diluted in 50 mM HEPES (pH 7.4) immediately before performing assays. The inhibition of hAcChE was determined using a 96-well plate assay based upon the original method described by Ellman [55, 56]. Reactions were performed in a total volume of 200 μl of 50 mM HEPES (pH 7.4) containing 1 mM acetylthiocholine, 0.5 mM 5,5′-dithio-bis(2-nitrobenzoic acid), 0.45 U/ml hAcChE (amphiphilic form isolated from human erythrocytes), and appropriate concentrations of inhibitor. Absorbance at 405 nM was determined at 15 s intervals for up to 2 min. All data analyses were performed in duplicate using a minimum of eight concentrations of inhibitor, and Ki values were calculated in an identical fashion to that described above. R^2 values for the curve fits exceeded 0.95.

Acknowledgments

We thank members of the Redinbo Laboratory, including J. Chrencik, E. Howard-Williams, T. Lesher, S. Sakai, R. Watkins, and Y. Xue for experimental assistance. Supported by N.I.H. Grants CA77340, DK62229, and CA98468, a Burroughs Wellcome Career Award in the Biomedical Sciences (M.R.R), and by N.I.H. Grants CA76202 and CA79763, the Cancer Center Core Grant CA21765, and the American Lebanese Syrian Associated Charities (P.M.P.).

Received: January 17, 2003
Revised: March 13, 2003
Accepted: March 18, 2003
Published: April 21, 2003

References

1. Wadkins, R.M., Morton, C.L., Weeks, J.K., Oliver, L., Weirdl, M., Danks, M.K., and Potter, P.M. (2001). Structural constraints affect the metabolism of 7-ethyl-10-[4-(1-piperidino)-1-piperidino]carbonyloxycamptothecin (CPT-11) by carboxylesterases. Mol. Pharmacol. *60*, 355–362.
2. Satoh, T., and Hosokawa, M. (1998). The mammalian carboxylesterases: from molecules to functions. Annu. Rev. Pharmacol. Toxicol. *38*, 257–288.
3. Harrison, E.H. (1998). Lipases and carboxylesterases: possible roles in the hepatic metabolism of retinol. Annu. Rev. Nutr. *18*, 259–276.
4. Satoh, T., Taylor, P., Bosron, W.F., Sanghani, S.P., Hosokawa, M., and La Du, B.N. (2002). Current progress on esterases: from molecular structure to function. Drug Metab. Dispos. *30*, 488–493.
5. Kamendulis, L.M., Brzezinski, M.R., Pindel, E.V., Bosron, W.F., and Dean, R.A. (1996). Metabolism of cocaine and heroin is catalyzed by the same human liver carboxylesterases. J. Pharmacol. Exp. Ther. *279*, 713–717.
6. Zhang, J., Burnell, J.C., Dumaual, N., and Bosron, W.F. (1999). Binding and hydrolysis of meperidine by human liver carboxylesterase hCE-1. J. Pharmacol. Exp. Ther. *290*, 314–318.
7. Alexson, S.E., Diczfalusy, M., Halldin, M., and Swedmark, S. (2002). Involvement of liver carboxylesterases in the in vitro metabolism of lidocaine. Drug Metab. Dispos. *30*, 643–647.
8. Tang, B.K., and Kalow, W. (1995). Variable activation of lovastatin by hydrolytic enzymes in human plasma and liver. Eur. J. Clin. Pharmacol. *47*, 449–451.
9. Takai, S., Matsuda, A., Usami, Y., Adachi, T., Sugiyama, T., Katagiri, Y., Tatematsu, M., and Hirano, K. (1997). Hydrolytic profile for ester- or amide-linkage by carboxylesterases pI 5.3 and 4.5 from human liver. Biol. Pharm. Bull. *20*, 869–873.
10. Bencharit, S., Morton, C.L., Xue, Y., Potter, P.M., and Redinbo, M.R. (2003). Structural basis of cocaine and heroin metabolism by a promiscuous human drug-processing enzyme. Nat. Struct. Biol., in press.
11. Brzezinski, M.R., Spink, B.J., Dean, R.A., Berkman, C.E., Cashman, J.R., and Bosron, W.F. (1997). Human liver carboxylesterase hCE-1: binding specificity for cocaine, heroin, and their metabolites and analogs. Drug Metab. Dispos. *25*, 1089–1096.
12. Brzezinski, M.R., Abraham, T.R., Stone, C.L., Dean, R.A., and Bosron, W.F. (1994). Purification and characterization of a human liver cocaine carboxylesterase that catalyzes the production of benzoylecgonine and the formation of cocaethylene from alcohol and cocaine. Biochem. Pharmacol. *48*, 1747–1755.
13. Diczfalusy, M.A., Bjorkhem, I., Einarsson, C., Hillebrant, C.G., and Alexson, S.E. (2001). Characterization of enzymes involved in formation of ethyl esters of long-chain fatty acids in humans. J. Lipid Res. *42*, 1025–1032.
14. Nanji, A.A., Su, G.L., Laposata, M., and French, S.W. (2002). Pathogenesis of alcoholic liver disease–recent advances. Alcohol. Clin. Exp. Res. *26*, 731–736.
15. Becker, A., Bottcher, A., Lackner, K.J., Fehringer, P., Notka, F., Aslanidis, C., and Schmitz, G. (1994). Purification, cloning, and expression of a human enzyme with acyl coenzyme A: cholesterol acyltransferase activity, which is identical to liver carboxylesterase. Arterioscler. Thromb. *14*, 1346–1355.
16. Ghosh, S. (2000). Cholesteryl ester hydrolase in human monocyte/macrophage: cloning, sequencing, and expression of full-length cDNA. Physiol. Genomics *2*, 1–8.
17. Mesange, F., Sebbar, M., Capdevielle, J., Guillemot, J.C., Ferrara, P., Bayard, F., Poirot, M., and Faye, J.C. (2002). Identification of two tamoxifen target proteins by photolabeling with 4-(2-morpholinoethoxy)benzophenone. Bioconjug. Chem. *13*, 766–772.
18. Ellgaard, L., Molinari, M., and Helenius, A. (1999). Setting the standards: quality control in the secretory pathway. Science *286*, 1882–1888.
19. Potter, P.M., Wolverton, J.S., Morton, C.L., Wierdl, M., and Danks, M.K. (1998). Cellular localization domains of a rabbit and a human carboxylesterase: influence on irinotecan (CPT-11) metabolism by the rabbit enzyme. Cancer Res. *58*, 3627–3632.
20. van Pelt, J.F., Moshage, H.J., Depla, E., Verhave, J.P., and Yap, S.H. (1997). Identification of human liver carboxylesterase as one of the proteins involved in Plasmodium falciparum malaria sporozoite invasion in primary cultures of human hepatocytes. J. Hepatol. *27*, 688–698.
21. Zhen, L., Rusiniak, M.E., and Swank, R.T. (1995). The beta-glucuronidase propeptide contains a serpin-related octamer necessary for complex formation with egasyn esterase and for retention within the endoplasmic reticulum. J. Biol. Chem. *270*, 11912–11920.
22. Yue, C.C., Muller-Greven, J., Dailey, P., Lozanski, G., Anderson,

V., and Macintyre, S. (1996). Identification of a C-reactive protein binding site in two hepatic carboxylesterases capable of retaining C-reactive protein within the endoplasmic reticulum. J. Biol. Chem. *271*, 22245–22250.

23. Labarrere, C.A., Lee, J.B., Nelson, D.R., Al-Hassani, M., Miller, S.J., and Pitts, D.E. (2002). C-reactive protein, arterial endothelial activation, and development of transplant coronary artery disease: a prospective study. Lancet *360*, 1462–1467.
24. Jann, M.W., Shirley, K.L., and Small, G.W. (2002). Clinical pharmacokinetics and pharmacodynamics of cholinesterase inhibitors. Clin. Pharmacokinet. *41*, 719–739.
25. Dvir, H., Wong, D.M., Harel, M., Barril, X., Orozco, M., Luque, F.J., Munoz-Torrero, D., Camps, P., Rosenberry, T.L., Silman, I., et al. (2002). 3D structure of Torpedo californica acetylcholinesterase complexed with huprine X at 2.1 A resolution: kinetic and molecular dynamic correlates. Biochemistry *41*, 2970–2981.
26. Dvir, H., Jiang, H.L., Wong, D.M., Harel, M., Chetrit, M., He, X.C., Jin, G.Y., Yu, G.L., Tang, X.C., Silman, I., et al. (2002). X-ray structures of Torpedo californica acetylcholinesterase complexed with (+)-huperzine a and (-)-huperzine B: structural evidence for an active site rearrangement. Biochemistry *41*, 10810–10818.
27. Sjogren, M., Hesse, C., Basun, H., Kol, G., Thostrup, H., Kilander, L., Marcusson, J., Edman, A., Wallin, A., Karlsson, I., et al. (2001). Tacrine and rate of progression in Alzheimer's disease—relation to ApoE allele genotype. J. Neural Transm. *108*, 451–458.
28. Tsolaki, M., Pantazi, T., and Kazis, A. (2001). Efficacy of acetylcholinesterase inhibitors versus nootropics in Alzheimer's disease: a retrospective, longitudinal study. J. Int. Med. Res. *29*, 28–36.
29. Sussman, J.L., Harel, M., and Silman, I. (1993). Three-dimensional structure of acetylcholinesterase and of its complexes with anticholinesterase drugs. Chem. Biol. Interact. *87*, 187–197.
30. Harel, M., Schalk, I., Ehret-Sabatier, L., Bouet, F., Goeldner, M., Hirth, C., Axelsen, P.H., Silman, I., and Sussman, J.L. (1993). Quaternary ligand binding to aromatic residues in the active-site gorge of acetylcholinesterase. Proc. Natl. Acad. Sci. USA *90*, 9031–9035.
31. Diller, D.J., Pohl, E., Redinbo, M.R., Hovey, B.T., and Hol, W.G. (1999). A rapid method for positioning small flexible molecules, nucleic acids, and large protein fragments in experimental electron density maps. Proteins *36*, 512–525.
32. Gilson, M.K., Straatsma, T.P., McCammon, J.A., Ripoll, D.R., Faerman, C.H., Axelsen, P.H., Silman, I., and Sussman JL. (1994). Open "back door" in a molecular dynamics simulation of acetylcholinesterase. Science. *63*,1276–1278.
33. Bartolucci, C., Perola, E., Cellai, L., Brufani, M., and Lamba, D. (1999). "Back door" opening implied by the crystal structure of a carbamoylated acetylcholinesterase. Biochemistry *38*, 5714–5719.
34. Mulder, M., Blokland, A., van den Berg, D.J., Schulten, H., Bakker, A.H., Terwel, D., Honig, W., de Kloet, E.R., Havekes, L.M., Steinbusch, H.W., et al. (2001). Apolipoprotein E protects against neuropathology induced by a high-fat diet and maintains the integrity of the blood-brain barrier during aging. Lab Invest. *81*, 953–960.
35. Camps, P., and Munoz-Torrero, D. (2001). Tacrine-huperzine A hybrids (huprines): a new class of highly potent and selective acetylcholinesterase inhibitors of interest for the treatment of Alzheimer's disease. Mini. Rev. Med. Chem. *1*, 163–174.
36. Hu, M.K., Wu, L.J., Hsiao, G., and Yen, M.H. (2002). Homodimeric tacrine congeners as acetylcholinesterase inhibitors. J. Med. Chem. *45*, 2277–2282.
37. de los Rios, C., Marco, J.L., Carreiras, M.D., Chinchon, P.M., Garcia, A.G., and Villarroya, M. (2002). Novel tacrine derivatives that block neuronal calcium channels. Bioorg. Med. Chem. *10*, 2077–2088.
38. Carlier, P.R., Chow, E.S.-H., Han, Y., Liu, J., Yazal, J.E., and Pang, Y.-P. (1999). Heterodimeric tacrine-based acetycholinesterase inhibitors: investigating ligand-peripheral site interaction. J. Med. Chem. *42*, 4225–4231.
39. Williams, P.A., Cosme, J., Sridhar, V., Johnson, E.F., and McRee, D.E. (2000). Mammalian microsomal cytochrome P450 monooxygenase: structural adaptations for membrane binding and functional diversity. Mol. Cell *5*, 121–131.
40. Watkins, R.E., Wisely, G.B., Moore, L.B., Collins, J.L., Lambert, M.H., Williams, S.P., Willson, T.M., Kliewer, S.A., and Redinbo, M.R. (2001). The human nuclear xenobiotic receptor PXR: structural determinants of directed promiscuity. Science *292*, 2329–2333.
41. Schumacher, M.A., Miller, M.C., Grkovic, S., Brown, M.H., Skurray, R.A., and Brennan, R.G. (2001). Structural mechanisms of QacR induction and multidrug recognition. Science *294*, 2158–2163.
42. Morton, C.L., and Potter, P.M. (2000). Comparison of Escherichia coli, Saccharomyces cerevisiae, Pichia pastoris, Spodoptera frugiperda, and COS7 cells for recombinant gene expression. Application to a rabbit liver carboxylesterase. Mol. Biotechnol. *16*, 193–202.
43. Danks, M.K., Morton, C.L., Krull, E.J., Cheshire, P.J., Richmond, L.B., Naeve, C.W., Pawlik, C.A., Houghton, P.J., and Potter, P.M. (1999). Comparison of activation of CPT-11 by rabbit and human carboxylesterases for use in enzyme/prodrug therapy. Clin. Cancer Res. *5*, 917–924.
44. Otwinowski, Z., and Minor, W. (1993). Data Collection and Processing. (Warrington, United Kingdom: Daresbury Laboratories,).
45. Navaza, J. (1994). AmoRe: an automated package for molecular replacement. Acta Crystallogr. A *50*, 157–163.
46. Brünger, A.T., Adams, P.D., Clore, G.M., DeLano, W.L., Gros, P., Grosse-Kunstleve, R.W., Jiang, J.S., Kuszewski, J., Nilges, M., Pannu, N.S., et al. (1998). Crystallography and NMR system: a new software suite for macromolecular structure determination. Acta Crystallogr. D *54*, 905–921.
47. Jones, T.A., Zou, J.Y., Cowan, S.W., and Kjeldgaard, M. (1991). Improved methods for building protein models in electron density maps and the location of errors in these models. Acta Crystallogr. A *47*, 110–119.
48. Read, R.J. (1986). Improved Fourier coefficients for maps using phases from partial structures with errors. Acta Crystallogr. A *42*, 140–149.
49. Kraulis, P.J. (1991). MOLSCRIPT: a program to produce both detailed and schematic plots of protein structures. J. Appl. Crystollogr. *24*, 946–950.
50. Esnouf, R.M. (1999). Further additions to MolScript version 1.4, including reading and contouring of electron-density maps. Acta Crystallogr. D *55*, 938–940.
51. Merritt, E.A., and Murphy, M.E.P. (1991). Raster3D version 2.0-a program for photorealistic molecular graphics. Acta Crystallogr. D *50*, 869–873.
52. Beaufay, H., Amar-Costesec, A., Feytmans, E., Thines-Sempoux, D., Wibo, M., Robbi, M., and Berthet, J. (1974). Analytical study of microsomes and isolated subcellular membranes from rat liver. I. Biochemical methods. J. Cell Biol. *61*, 188–200.
53. Potter, P.M., Wolverton, J.S., Morton, C.L., Wierdl, M., and Danks, M.K. (1998). Cellular localization domains of a rabbit and a human carboxylesterase: influence on irinotecan (CPT-11) metabolism by the rabbit enzyme. Cancer Res. *58*, 3627–3632.
54. Cheng, Y., and Prusoff, W.H. (1973). Relationship between the inhibition constant (K1) and the concentration of inhibitor which causes 50 per cent inhibition (I50) of an enzymatic reaction. Biochem. Pharmacol. *22*, 3099–3108.
55. Ellman, G.L., Courtney, K.D., and Featherstone, R.M. (1961). A new and rapid colorimetric determination of acetylcholinesterase activity. Biochem. Pharmacol. *7*, 88–95.
56. Doctor, B.P., Toker, L., Roth, E., and Silman, I. (1987). Microtiter assay for acetylcholinesterase. Anal. Biochem. *166*, 399–403.

Accession Numbers

Atomic coordinates and structural factors for hCE1 in complex with tacrine have been deposited with the RCSB (accession code 1MX1).